Room Temperature Fluorescent Conjugated Polymer Gums

Young-Jae Jin, Jung-Eun Bae, Kwang-Soo Cho, Wang-Eun Lee, Dong-Yeon Hwang, and Giseop Kwak**

High molecular weight poly(diphenylacetylene) [PDPA] derivatives are introduced as fluorescent, soft conjugated polymers that exist in the gum state at room temperature. The gum-like behavior of the polymers is easily modified according to the side alkyl chain length and substitution position. Long alkyl chain-coupled PDPA derivatives provide soft and sticky gums at room temperature. Manual kneading of gum polymers produce soft films with very smooth surfaces. The gum polymers show an endothermic transition due to the melting of long alkyl chains. The X-ray diffraction of gum polymers reveals a new signal due to the molten aliphatic chains. The gum polymers show significant viscoelastic relaxation at the melting temperature of the alkyl side chains. The dynamic thermo-mechanical analysis (DTMA) of gum polymers at room temperature suggest that the meta-substituted polymer is softer and stickier than para-polymer. Rheological analysis suggests that the meta-polymer has less entanglement than para-polymer. The fluorescence emission of gum polymer is quite intense in the film and solution. The gum polymer film is readily stretched to produce a uniaxially oriented film. Stretching and subsequent relaxation of elastomer-supported gum polymer film generate buckles perpendicular to the axis of strain. The gum polymer film accommodates the large strain without cracking and delamination.

1. Introduction

Softened bulk products of organic chromophores and ionic compounds have attracted considerable interest because of their unexpected properties, novel functions, easy-to-process, and novel applications.[1] Recently, room-temperature liquid-organic-fluorophores based on π-conjugated molecule oligo(phenylenevinylene) have been developed.[2] These liquid compounds have many benefits, such as high electron density, intrinsic transparency, nonvolatility, and solvent-free condition processing, to serve as a fluorescent matrix for other components in white light-emitting composite systems. In this regard, softening the generally stiff and rigid rod-like π-conjugated polymers to gums or oils at room temperature without decreasing their molecular weights to the monomer or oligomer level is a considerable challenge for novel optoelectronic applications. On the other hand, conventional π-conjugated polymers, such as polythiophene, polyfluorene, polyphenylene, polyphenylenevinylene, and polyphenyleneethynylene, have planar geometries and strong intermolecular interactions due to the extremely stiff and rigid main chains, resulting in a highly cofacial chain packing in the solid state.[3] Although such a stacked chain structure is essential for effective intermolecular charge-carrier transport in the active layer within thin-film organic optoelectronic devices,[4] a cofacial packing structure is not preferable for high quantum efficiency and softness in the bulk solid state because it produces crystal domains, leading to significant self-quenching because the intermolecular excimers have an extremely low transition energy in a nonradiative process.[5] Although the attachment of a long alkyl side chain to the backbone, which results in a so-called "hairy-rods" structure, can enhance the solubility and charge-carrier mobility of the polymers, it is insufficient to collapse the cofacial chain packing structure.[6] Therefore, the crystal domains remain unchanged or grow preferentially, resulting in weak solid-state emission. Accordingly, the molecular design of highly emissive and intrinsically soft conjugated polymers in the solid state is one of the most attractive issues in advanced organic devices. In particular, if soft conjugated polymers are used in combination with elastomeric rubber matrices, they will be the key material for stretchable electronics.[7]

Very unusually, poly(diphenylacetylene) [PDPA] derivatives have a highly twisted backbone due to steric repulsion between the two bulky phenyl groups. Hence, its backbone is essentially non-coplanar with side phenyl rings.[8] Consequently, the PDPA derivatives are worm–like chain molecules with a relatively weak intermolecular interaction and non-planar geometry, which can lead to an unstacked chain conformation in the solid state. Moreover, PDPA derivatives are intensively fluorescent over a wide visible region from sky blue to greenish yellow due to intramolecular excimer emission resulting from a highly efficient exciton confinement between the bulky side phenyl rings.[9] In particular, unlike the cases of conventional

Y.-J. Jin, J.-E. Bae, Prof. K.-S. Cho, D.-Y. Hwang, Prof. G. Kwak
Department of Polymer Science and Engineering
Kyungpook National University
1370 Sankyuk-dong, Buk-ku, Daegu, 702–701, Korea
E-mail: polphy@knu.ac.kr; gkwak@knu.ac.kr
Dr. W.-E. Lee
Advanced Photonics Research Institute
Gwangju Institute of Science and Technology
1 Oryong-dong, Buk-gu, Gwangju, 500–712, Korea

DOI: 10.1002/adfm.201302829

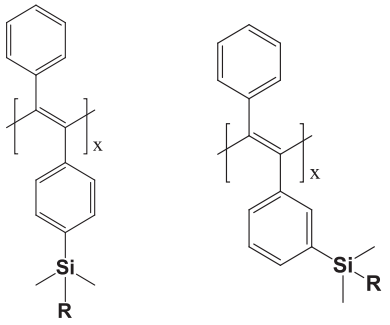

pC1 : R = Methyl **mC1** : R = Methyl
pC18 : R = Octadecyl **mC18** : R = Octadecyl

Scheme 1. Chemical structures of the poly (diphenylacetylene) [PDPA] derivatives.

conjugated polymers, the introduction of long alkyl side chain to PDPA derivatives leads to significantly improved emission quantum efficiency.[10] This has been attributed to the long alkyl side group acting as a plasticizer in the solid state to relax the intramolecular phenyl-phenyl stack structure effectively owing to the less dense chain packing structure.[11] Moreover, the PDPA derivative containing an extremely long alkyl side chain, such as an octadecyl group (pC18 in **Scheme 1**), was found to be quite soft and somewhat sticky, even though its physical features and mechanical/rheological properties have not been examined in detail.[11a]

Have you ever heard gum-like π-conjugated polymers? Here we introduce high molecular weight PDPA derivatives as fluorescent, soft conjugated polymers that exist in the gum state at room temperature. The gum-like behavior of the polymers was modified easily according to the side alkyl chain length and substitution position. This paper provides details of their unique thermodynamic, thermomechanical, rheological, and photophysical properties. Some of the PDPA derivatives should be a promising candidate material for highly fluorescent and very soft π-conjugated polymer gums that are potentially applicable to stretchable optoelectronic devices.

2. Result and Discussion

The molecular design of PDPA derivatives, including the chain length and substitution position of the side alkyl group, was very important for determining the physical features of the product polymers. The long alkyl chain-coupled PDPA derivatives (pC18 and mC18 in Scheme 1) provided soft and sticky gums at room temperature, whereas short alkyl chain-containing PDPA derivatives (pC1 and mC1 in Scheme 1) were obtained as glassy solids. The gum polymers were purified by Soxhlet extraction with methanol and acetone sequentially several times to afford yellow (pC18) and orange (mC18) gums in high yield (>70%). The weight average molecular weights (M_w) of pC18 and mC18 were extremely high, 8.7×10^5 (PDI 1.31) and 8.0×10^5 g mol^{-1} (PDI 1.63), respectively (Table S1, Supporting Information). These quantitative yields and high molecular weights, even after Soxhlet extraction, indicate the absence of residual solvent and low molecular weight impurities in the bulk materials. Therefore, the gum-like behavior is an inherent property of the single bulk component. The gummy solids of pC18 and mC18 produced featured films through not only conventional film-preparation methods of solvent casting and spin-coating but also a consecutive mechanical process. Manual kneading and pressing of the polymer gums produced soft films with very smooth surface (**Figure 1**a and Movie S1, Supporting Information). In contrast, the glassy polymers of pC1 (M_w:13.4×10^5; PDI: 1.16) and mC1 (M_w:11.7×10^5; PDI: 1.43) did not form such a soft film after the same processing, but left powdery materials (Figure 1a). In particular, when a thick mC18 film was compressed manually using an acryl resin stamp, it gave a completely clogged, three-dimensionally featured film in a well-defined pattern, as shown in Figure 1b. The reason for this is that mC18 is softer than pC18 because of its lower storage modulus (E') of mC18 (13.3 MPa) at room temperature than that of pC18 (53.7 MPa). Moreover, mC18 was much stickier than pC18. Owing to the adhesive behavior, the mC18 film stuck rapidly to a smooth surface (glass) and even to a highly porous, rough surface (paper) (Figure 1c and Movie S1, Supporting Information). This suggests that the substitution position of the alkyl side chain as well as the alkyl chain length is an important factor for making the PDPA derivative a softer and stickier gum-like polymer. Details of the thermomechanical and rheology analysis will be described later.

The polymer gums of pC18 and mC18 were evaluated by differential scanning calorimetry (DSC) and compared with the corresponding glassy polymers. As shown in **Figure 2**, the heating traces in the DSC thermogram indicate that both gum

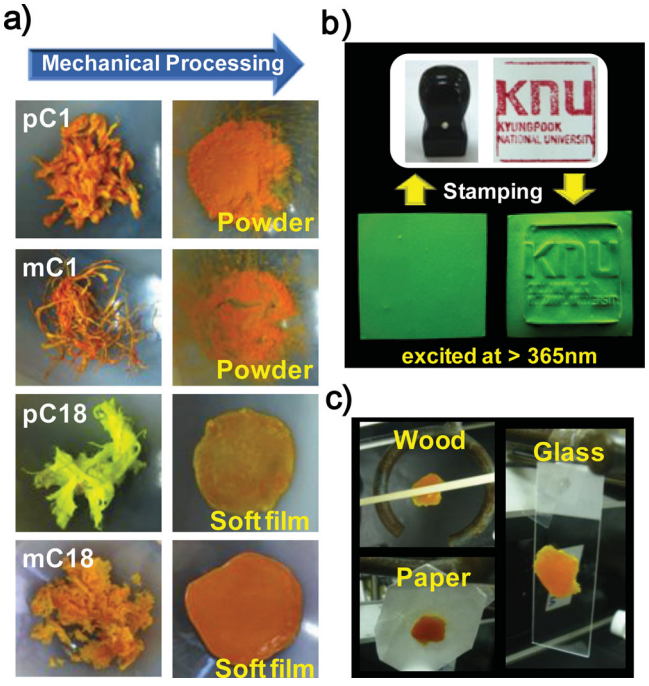

Figure 1. a) Changes in the physical features of PDPA derivatives by kneading and subsequent roll-pressing. b) Fluorescent images of the free-standing mC18 film (prepared by solvent casting method, thickness >20 μm, excited at >365 nm) before and after compression with acryl-resin stamp. c) Adhesive behavior of the mC18 film on the surfaces of glass, wood, and paper.

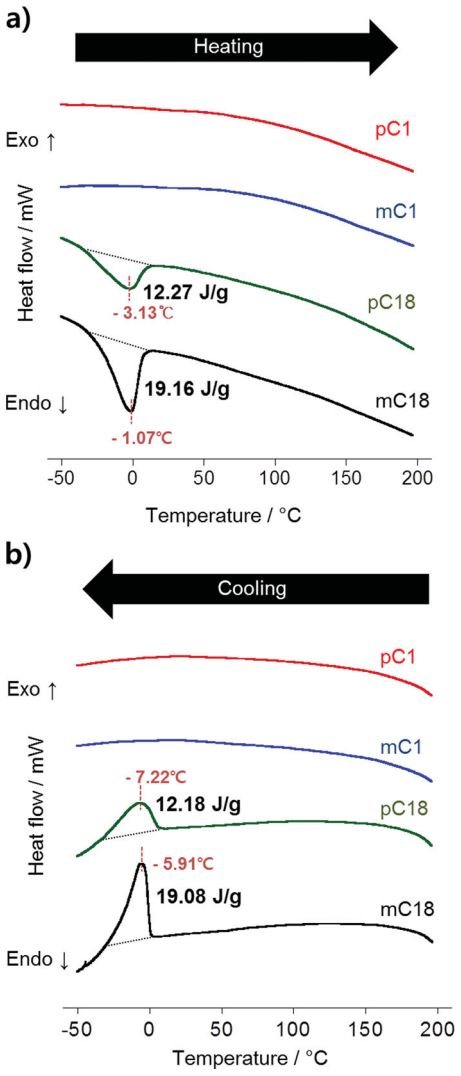

Figure 2. DSC thermogram of PDPA derivatives on a) heating and b) cooling process (heat flow rate ≈10 °C min^{-1}, under nitrogen gas).

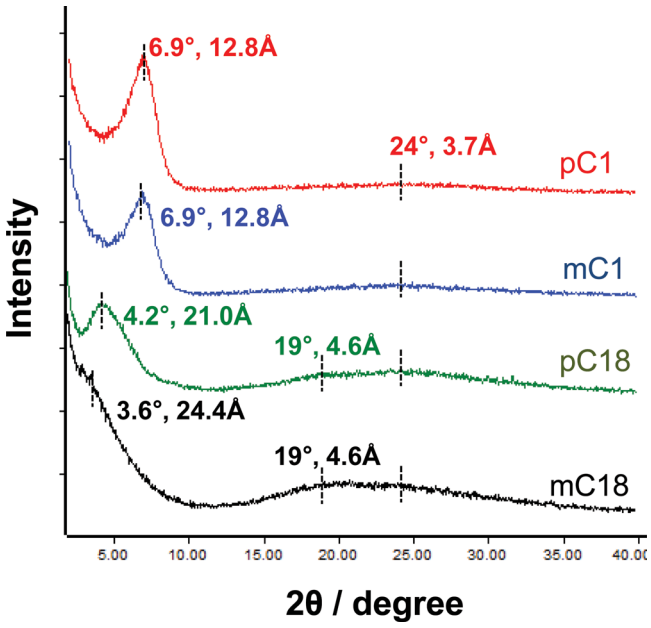

Figure 3. Wide-angle X-ray diffraction (WAXD) patterns of the PDPA derivatives in solvent-cast films at room temperature.

polymers have relatively low thermodynamic transition temperatures of approximately –2 °C due to an endothermic volume change, whereas the short alkyl chain-containing glassy polymers, pC1 and mC1, showed no transition over a wide range of –50 to 200 °C. Accordingly, the endothermic peaks at approximately –2 °C should be due to melting of the side chain octadecyl groups in the bulk solid. Moreover, in the cooling process, the gum polymers apparently showed an exothermic transition at a lower temperature (ca. –6 °C) due to crystallization of the alkyl side chains. On the other hand, the melting temperature (T_m) of octadecane was 28 °C. Consequently, the lower transition temperature of the side chain octadecyl group relative to the crystalline hydrocarbon should be because of the weakened intermolecular force due to the longer distance between the side chains attached to the highly twisted backbone. The enthalpy of fusion (ΔH_{fus}) for the octadecyl chains in pC18 and mC18 was determined to be 12.3 and 19.2 J g^{-1}, respectively, whereas the ΔH_{fus} of octadecane was 241.6 J g^{-1}.[12] From these ΔH_{fus} values, the degrees of crystallinity of the alkyl side chains in pC18 and mC18 were calculated to be 5.0 and 7.9%, respectively, indicating a higher degree of crystallinity in mC18 rather than in pC18. This might be because the meta-polymer has a highly stable and regular intramolecular phenyl-phenyl stack structure in a continuous helical manner, whereas the para-polymer has a randomly dispersed phenyl-phenyl stack structure in a discontinuous zigzag pattern.[11b] Consequently, the higher degree of crystallinity of the alkyl side chains in mC18 should be due to a better-ordered arrangement along with the regularly stacked side phenyl rings.

The disordered amorphous structures of the gum polymers at room temperature were determined by X-ray diffraction (XRD) and compared with the corresponding glassy polymers (**Figure 3**). Both glassy polymers of pC1 and mC1 showed a sharp signal at a small angle of 6.9° due to the lamellar layer, which corresponds to a distance of approximately 12.8 Å according to the Bragg equation, whereas the small angle diffraction peaks of pC18 and mC18 appeared at a lower angle of 4.2° and 3.6°, respectively, corresponding to a distance of approximately 21.0 Å and 24.4 Å, respectively. The broad scattering signals were also observed over a wide angle region for the present polymers, indicating that these polymers are basically amorphous. The glassy polymers showed a roughly single peak at ≈24°(3.7 Å), whereas the gum polymers showed a new signal at ≈19°(4.6 Å) in addition to a peak at 24°. The 3.7 Å distance corresponds to the mean π–π stack distance of the side phenyl rings whereas the 4.6 Å distance corresponds to the mean distance of the molten aliphatic chains.[13] The integral peak intensity ratios of $I_{4.2°}/I_{24°}$ for pC18 and $I_{3.6°}/I_{24°}$ for mC18 were calculated to be approximately 3, which are much smaller than the $I_{6.9°}/I_{24°}$ ratio (about 10) for glassy polymers. This suggests that the ordered lamellar structure of PDPA derivatives in the bulk solid had been partially collapsed by the extremely long alkyl chains and the amorphous phase increased slightly more.

This should be because the molten long alkyl chain groups act as plasticizers to reduce the interchain interactions and increase the degree of molecular disorder in the bulk system.

DSC and XRD revealed the importance of the highly twisted backbone and long alkyl side chain of pC18 and mC18 in the bulk solid in molecular design strategy for room temperature gum-like conjugated polymer in terms of the thermodynamic relaxation transition and disordered phases. Considering the DSC and XRD results, viscoelastic relaxation is expected at the melting temperature of the long alkyl side chains. **Figure 4** shows dynamic thermo-mechanical analysis (DTMA) data of the four polymers. The loss modulus (E'') of pC1 and mC1 do not show any peak in the temperature range, –40 to 40 °C. On the other hand, both pC18 and mC18 show a strong viscoelastic relaxation peak at the melting temperature of the alkyl side chains, as expected from the DSC data.

Although the main chains of pC18 and mC18 are expected to remain in the glassy state, even after the melting of long alkyl side chains, the high-mobility region generated by melting reduces the storage modulus (E') dramatically. As the temperature was increased, the E's of both pC18 and mC18 showed a plateau of approximately 33 and 2.5 MPa, respectively. It is reported that the values of plateau modulus of flexible polymers are in the range, 0.2 to 2.6 MPa.[14] The plateau modulus of a molten polymer is known to correspond to the modulus of a rubbery polymer network formed by entanglements. Because the origin of the plateau modulus is conformation entropy rather than the energies for chain torsion and interchain interactions, more flexible chains, such as polyethylene (PE) or polybutadiene (PBD), shows a higher plateau modulus (2.6 and 1.25 MPa, respectively) than the less flexible chains, such as polystyrene (PS) and polymethylmethacrylate (PMMA) (0.2 and 0.3 MPa, respectively). The plateau modulus of both pC18 and mC18 are higher than those of PE and PBD even though the main chains of pC18 and mC18 have more rigid structures compared to PS and PMMA. This suggests that the origins of the plateau modulus of pC18 and mC18 appear like a combination of the relatively low temperature relaxation transition and disordered phases of the polymer chains as already described in DSC and XRD results. Consequently, melting of the side chains endows pC18 and mC18 with rubber-like mechanical properties at room temperature. In particular, the plastic deformation

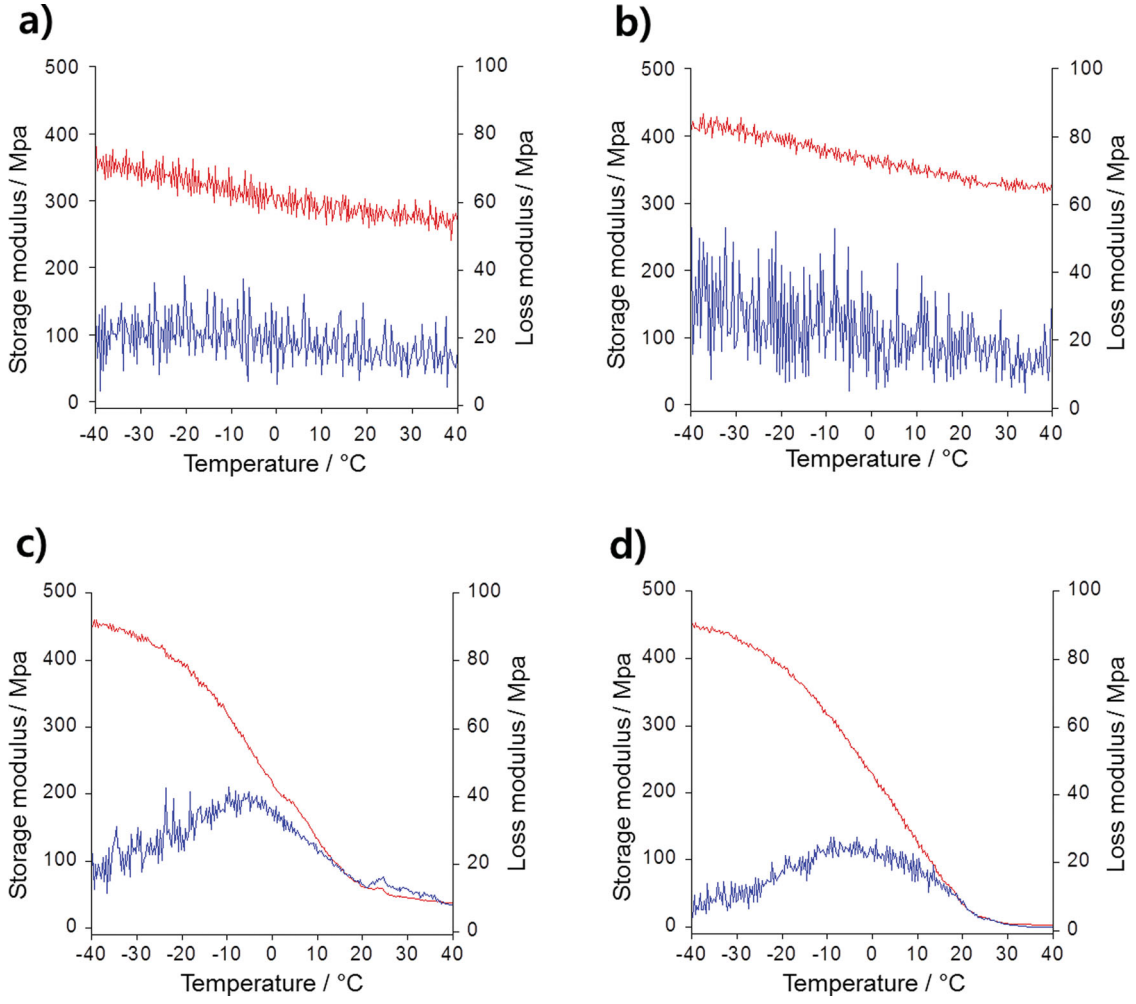

Figure 4. DTMA of the PDPA derivatives (Initiated force: 0.05N at frequency 1 Hz; Heating rate: 10 °C min^{-1} under nitrogen gas): a) pC1, b) mC1, c) pC18, d) mC18, storage modulus (red), loss modulus (blue).

(permanent strain) due to stamping (Figure 1) suggests that the structure of mC18 at room temperature is totally different from general rubber materials. Elastic recovery of rubber materials originates from the junction points between the flexible chains. On the other hand, plastic deformation implies that relative positions of the chains are changed after large deformation due to slippage between the chains. Therefore, the permanent strain after the stamping of mC18 can be explained by the melting region between the rigid main chains.

The PDPA derivatives are known to have large fractional free volumes (FFV).[15] Generally, the modulus of glassy polymers is in the GPa range. The *E'* values at the lowest temperature (–40 °C) of the PDPA derivatives are in the MPa range, which are much lower than those of conventional glassy polymers. These lower values reflect the large FFVs of PDPA derivatives very well. Interestingly, the *E'* values of pC1 and mC1 at –40 °C were lower than those of pC18 and mC18. This can be explained by the long alkyl side chains forming rigid crystals below the melting temperature, whose modulus is higher than that of the glassy regions of the backbone chains. Accordingly, the long side alkyl chains form strong anchors below the melting point, whereas the side alkyl chains play the role of lubricants in the slippage of rigid main chains over the melting point. This supports the idea that the long alkyl side chains weaken the interchain interaction to plasticize the stiff and rigid polymer backbones effectively at room temperature.

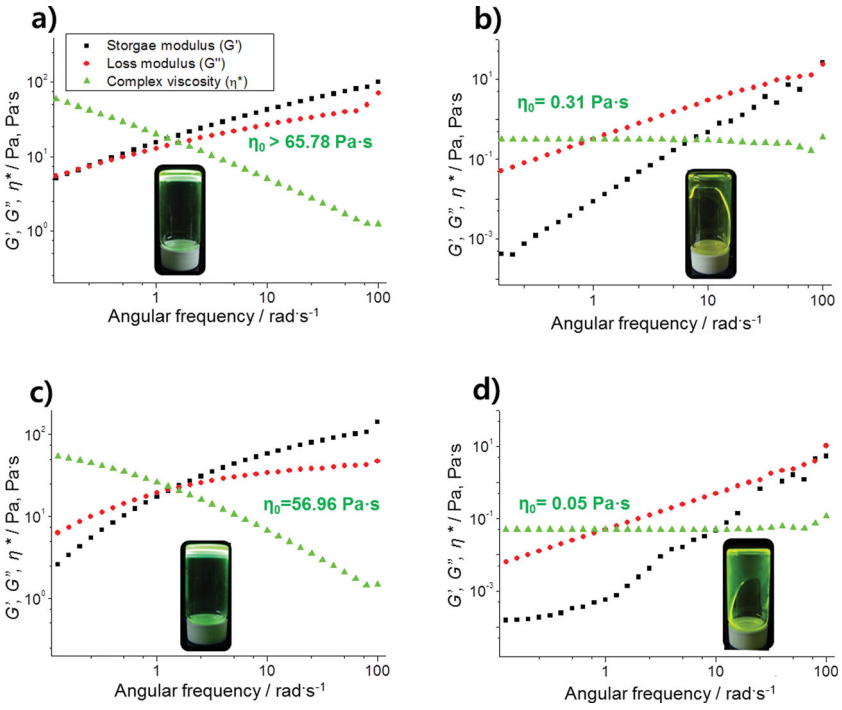

Figure 5. Log-log plots of the shear dynamic modulus of the polymer solutions as function of the angular frequency (1,2-dichlorobenzene solution, concentration 5×10^{-2} M): a) pC1, b) mC1, c) pC18, d) mC18. Inset: FL photographs (excited at >365 nm).

It should be also noted that the difference in the dynamic mechanical properties between the para- and meta-polymers is dependent on whether the polymer is a gum or glassy. That is, for the glassy polymers at room temperature, the meta-polymer (mC1, *E'* 330.6 MPa) was stiffer and more rigid than the para-polymer (pC1, *E'* 280.5 MPa), whereas for the gum polymers, the meta-polymer (mC18, *E'* 2.5 MPa) was softer and stickier than the para-polymer (pC18, *E'* 33.0 MPa). The comparative main chain rigidity of the glassy polymers can be estimated from the fact that mC1 has a much higher viscosity index (α = 1.07 in THF at 40 °C, where α value is defined as the Mark-Houwink-Sakurada equation, $[\eta] = KM^{\alpha}$) than pC1 with an α value of 0.80.[11b] Therefore, it is reasonable to think that the elastic modulus of the glassy polymers is mainly dependent on the main chain rigidity. However, the difference in elastic modulus between mC18 and pC18 could not be explained by the main chain rigidity because the meta-polymer was softer than para-polymer. In such unusual quasi-solid states of the rigid conjugated polymers of which the molten side alkyl chains act as a plasticizer in the bulk solid, chain entanglement would be a more dominant than the chain rigidity for determining the softness and stickiness of the bulk solid. That is, as the chain entanglement decreases, the softness of such a gum-like polymer in a bulk solid might increase further.[16]

Therefore, this study examined the rheological properties of all the present polymers. Surprisingly, both para-polymer (pC1 and pC18) solutions exhibited gel-like behavior, whereas both meta-polymer (mC1 and mC18) solutions were flowing down, as shown in the inset in **Figure 5**. Figure 5 shows the linear viscoelasticity of the PDPA derivatives in highly concentrated dichlorobenzene solutions (concentration 5.0×10^{-2} mol L^{-1} in repeat unit). Over the frequency range, 0.1–100 rad Pa s^{-1}, and at a shear strain of $\gamma = 0.1$, the complex viscosities of both mC1 and mC18 were nearly independent of the frequency, whereas those of pC1 and pC18 showed shear thinning. In terms of the dynamic moduli, mC1 showed fully developed terminal behavior, where the storage modulus (*G'*) is proportional to the square of the frequency and the loss modulus (*G"*) is proportional to the frequency. The strange frequency dependence of the *G'* of mC18 is due to the much lower elasticity, which is contaminated by noise, whereas the *G"* of mC18 shows clear terminal behavior. On the other hand, pC1 and pC18 do not show terminal behavior. The linear viscoelasticity of pC18 in this frequency region exhibited plateau behavior rather than terminal behavior. Figure 5 shows that the order of relaxation time is pC1 > pC18 > mC1 > mC18, which is the same order observed for the zero-shear viscosity (η_0). The η_0 of pC1, pC18, mC1 and mC18 in the concentrated solution were determined to be >65.8, 56.9, 0.31, and 0.05 Pa s, respectively. This clearly suggests that the meta-polymers have less entanglement than the para-polymers. The less entanglement of mC18 relative to pC18 was also confirmed by the fact that mC18 promptly dissolved in hexane upon contact, whereas despite the structural similarity and similar M_w between the two polymers, pC18

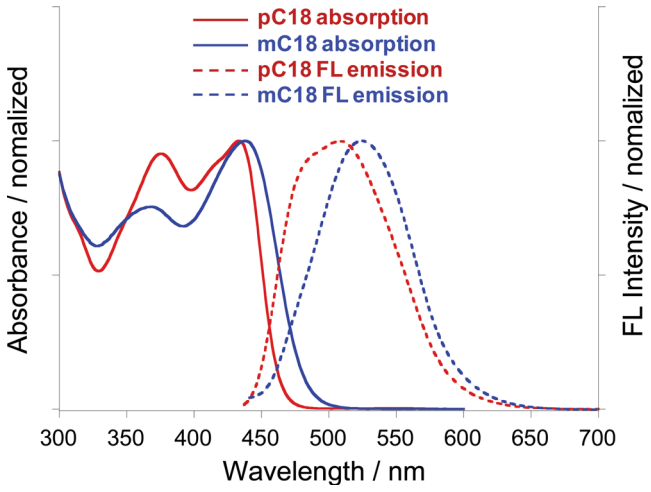

Figure 6. UV-vis absorption and FL emission spectra (excited at 420 nm) of pC18 and mC18 in solution (1×10^{-5} M, in toluene).

did not readily dissolve in the same solvent but dissolved very slowly over several days. Basically, these gum-like polymers have almost no interchain interactions except for the very weak Van der Waals force. Accordingly, mC18 should have a much greater degree of molecular slipping and lower cohesive energy in the bulk solid due to less entanglement as compared to pC18 with much more entanglement. This chain entanglement effect can explain why the mC18 is softer and stickier than pC18.

From the view point of the development of a soft conjugated polymer, the entanglement effect is still interesting. Therefore, it will be important to discuss the original reason for the difference in the degree of chain entanglement between the para- and meta-polymers. The less entanglement of the meta-polymer should be due to the more extended chain structure relative to the para-polymer. This was strongly supported by UV-vis absorption and fluorescence (FL) emission spectroscopy. As shown in **Figure 6**, the UV-vis absorption maximum band ($\lambda_{max,abs}$) of mC18 in an ideal solution showed a 4 nm shift to a longer wavelength of 437 nm compared to pC18 (433 nm). Moreover, the FL emission maximum band ($\lambda_{max,em}$) of mC18 appeared at a much longer wavelength of 525 nm compared to pC18 (507 nm). As definite evidence, pC18 apparently showed a monomer emission band at approximately 470 nm due to the kink structure of the polymer segments, whereas the mC18 did not. This suggests that mC18 has a more rigid main chain than pC18, which corresponds to the results of the viscosity indices of the glassy polymers of pC1 and mC1.

Figure 7 summarizes the comparative physical features of all the present polymers. The alkyl side chain length is responsible for the plasticizer effect, whereas substitution position is responsible for the chain entanglement and rigidity. The mC18 is the softest polymer due to the plasticizer effects of the molten alkyl side chain and less entanglement in the disordered bulk phase, whereas mC1 is the hardest polymer due to the main chain rigidity and less entanglement in the ordered bulk phase.

The gum-like behavior and disordered amorphous structure of the longer alkyl chain-coupled PDPA derivatives were reflected in their photophysical properties. **Figure 8** shows the FL emission spectra and emission color photographs of the softest polymer (mC18) in both the bulk solid and solution compared to the hardest polymer (mC1). The $\lambda_{max,em}$ of mC18 in solution and gum film was similar (526 nm in a toluene solution and 528 nm in the spin-coated film), even though the full-width-at-half-maximum (FWHM) was slightly narrower in the bulk solid than in solution. Moreover, the FL emission of mC18 was quite intense in the film and ideal solution (Supporting Information, Table S2: quantum emission yield Φ_{em} = 5.58% in solution; 5.56% in film; average FL lifetime τ_{avr} = 0.211 ns in solution; 0.576 ns in film). The insets show images of mC18 in film and solution at room temperature under a hand-held UV lamp (λ_{ex} > 365 nm). The intense emission could be observed by the naked eye. In contrast, the FL emission of mC1 was weak in solution and almost quenched in the film (Supporting Information, Table S2: Φ_{em} = 1.19% in solution; 0.23% in film; τ_{avr} = 0.076 ns in solution; 0.176 ns in film). Unlike the case of mC18, mC1 in bulk solid and solution showed significantly different $\lambda_{max,em}$. The FL emission band of mC18 in solution was noted at a slightly shorter wavelength ($\lambda_{max,em}$ 525 nm) relative to that (526 nm) of mC1 in solution, whereas the FL emission band of mC18 in film

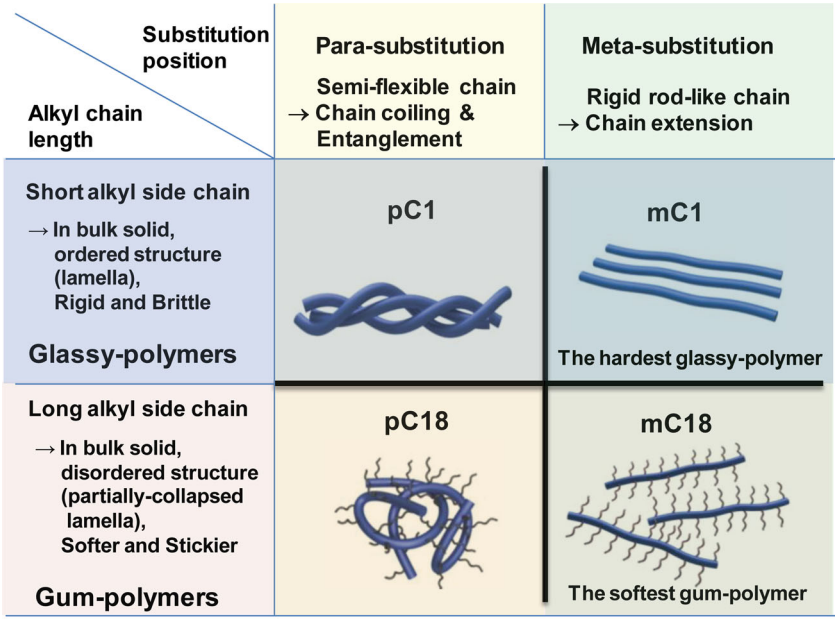

Figure 7. Schematic diagram of the effects of the alkyl side chain length and its substitution position on the softness of PDPA derivatives in a bulk solid.

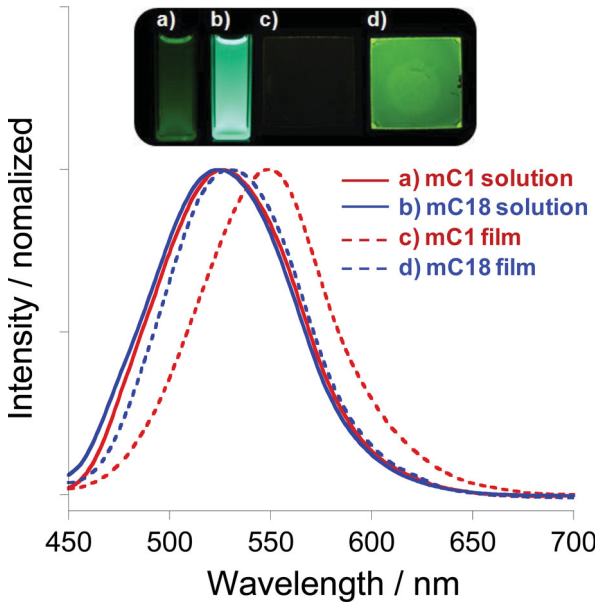

Figure 8. FL emission spectra of mC1 and mC18 in solution (1×10^{-5} M in toluene) and bulk solid (spin-coated film, thickness ≈200 nm) (excited at 420 nm). Inset: FL photographs (excited at >365 nm).

shifted to a much shorter wavelength ($\lambda_{max,em}$ 528 nm) compared to that (550 nm) of the mC1 film.

To explain the reason why the gum-like mC18 film showed significantly enhanced FL emission quantum efficiency and a blue shift relative to the glassy mC1 film, the FL origin of these PDPA derivative polymers should be considered. The difference in the FL emission properties between these two polymers should not be correlated with the intermolecular excimer generation because both polymers are totally unstacked in the solid state. Their FL emission is based on the intramolecular excimer species, which arises from side phenyl-phenyl stacking.[11] In general, FL emission becomes weaker with increasing degree of the stack structure. As mentioned previously, the side phenyl-phenyl stack structure can be relaxed by the long alkyl side chains because the molten alkyl groups at room temperature can act as a plasticizer in the bulk solid. Accordingly, the higher emission quantum efficiency and blue-shift of the gum-like mC18 compared to the glassy mC1 should be due to a highly relaxed side phenyl-phenyl stack structure with a higher electronic π–π^* transition energy in a radiative process.

Recently, highly polarized FL emissive conjugated polymers have attracted considerable attention because of their potential applications in the fields of organic light-emitting devices.[17] Highly anisotropic films can be obtained by carefully controlling the solid-state morphology via mechanical processing as well as molecular design. In this study, when the mC18 film (free-standing, thickness ≈20 µm) was drawn manually, it was stretched approximately 2 times in length to the maximum to produce a uniaxially oriented film (**Figure 9**a). As expected, however, the glassy polymers of pC1 and mC1 were not stretched. Figures 9b and 9c show the polarized UV-vis absorption and FL emission spectra of the oriented mC18 film. The parallel and perpendicular components in absorption were significantly different from each other (Figure 9b). The 430 nm absorption band due to the π–π^* transition of the polymer backbone reached a maximum intensity in the direction parallel to

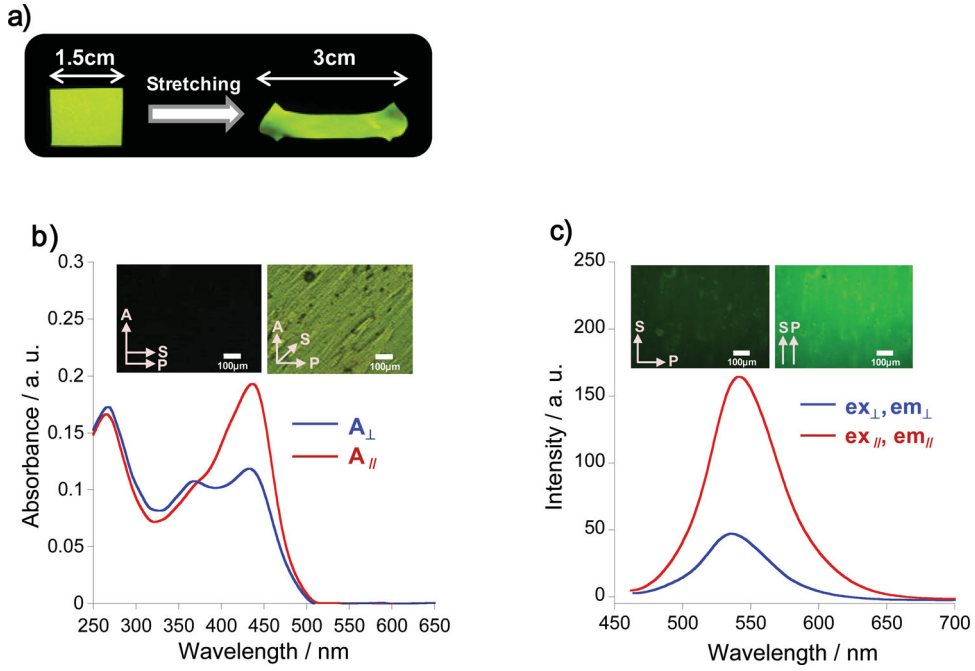

Figure 9. a) Stretching of the free-standing mC18 film (thickness ≈20 µm), b) Polarized UV-vis absorption ($A_{//}$: absorption parallel; $A_{\perp}$: absorption perpendicular to stretching direction) and c) polarized FL emission spectra (excited at 420 nm, $ex_{//}$: excited at 0°; $em_{//}$: monitored at 0°; $ex_{\perp}$: excited at 90°; $em_{\perp}$: monitored at 90°) of the stretched mC18 free-standing film. Insets: polarized optical microscopy image in b), polarized FL microscopy image (excited at >365 nm) in c). The script "A", "S", "P" indicates the analyzer direction, stretching direction, and polarizer direction, respectively.

the stretching direction, whereas the 370 nm band due to the localized electrons in the side phenyl rings reached a maximum in the perpendicular direction. This suggests that the polymer chains had aligned in a direction parallel to the stretching direction. To evaluate the degree of polymer chain alignment, the optical order parameter (S) was calculated using the following equation: $S = (D_{abs} - 1)/(D_{abs} + 2)$, where D_{abs} is the apparent dichroic ratio of absorption ($A_{//}/A_{\perp}$). If the molecular axes are ideally parallel and perpendicular to the stretching directions, the S value will be 1.0 and –0.5, respectively. The polarized absorption spectra revealed $D_{abs} = 1.63$ at 430 nm. Therefore, the S value was calculated to be 0.17, which is closer to the ideal value of 1.0 rather than –0.5, confirming that the polymer chain prefers to align along the direction parallel to the stretching direction. The FL emission in the parallel direction ($em_{//}$: monitored at 0°; $ex_{//}$: excited at 0°) was much more intense, approximately 3.5 times than that in the perpendicular direction ($em_{\perp}$: monitored at 90°; $ex_{\perp}$: excited at 90°), suggesting that the oriented mC18 film has highly polarized FL emission (Figure 9c). The optical anisotropy of the oriented mC18 film was also confirmed by polarizing optical microscopy (POM) and polarizing FL microscopy (PFM), as shown in the insets. Also, when the monitored wavelength was varied in the range of 450–650 nm, the polarized excitation spectra of stretched mC18 film in the parallel and perpendicular direction were almost identical to each other in the spectral shape (Figure S1, Supporting Information). This indicates that the emission of the stretched polymer film comes from same luminescent photoexcited species, irrespective of polarizing direction.

Elastomeric rubbers can serve as matrices or substrates to impart elasticity under tensile strain as well as flexibility to intrinsically rigid materials, which has led to the outstanding recent developments of stretchable optoelectronic devices.[18] As mentioned above, mC18 was stretched readily using the drawing method to exhibit great optical anisotropy. On the other hand, the polymer film did not return to its initial state due to the lack of elasticity. To make the film stretch and relax reversibly, an elastomer-supported film (film thickness ≈200 nm) was prepared by spin-coating a mC18 solution on a PDMS substrate. A mC1 film (film thickness ≈200 nm) was also prepared using the same method to compare with the mC18 film. In general, a buckling phenomenon occurs when compressive strain is applied to a system consisting of a rigid film on an elastomeric substrate.[19] The as-prepared, rigid mC1 film apparently exhibited buckles with disordered waves on the PDMS substrate due to the intrinsic rigidity, whereas the mC18 film showed no regular features, presumably due to the intrinsic softness (**Figure 10**a). After stretching (strain of 200%) and subsequently relaxing the films several ten times, both polymer films showed newly generated buckles perpendicular to the axis of strain (Figure 10b). The mC1 film, however, produced many cracks and was ultimately delaminated from the PDMS substrate. On the other hand, mC18 film accommodated a large strain without cracking and delamination, even after several hundred repetitions of the stretching and relaxing process. Similar to the free-standing mC18 film, the elastomer-supported mC18 film showed great optical anisotropy in UV-vis absorption (S value ≈0.19) and FL emission when stretched (Figure 10c).

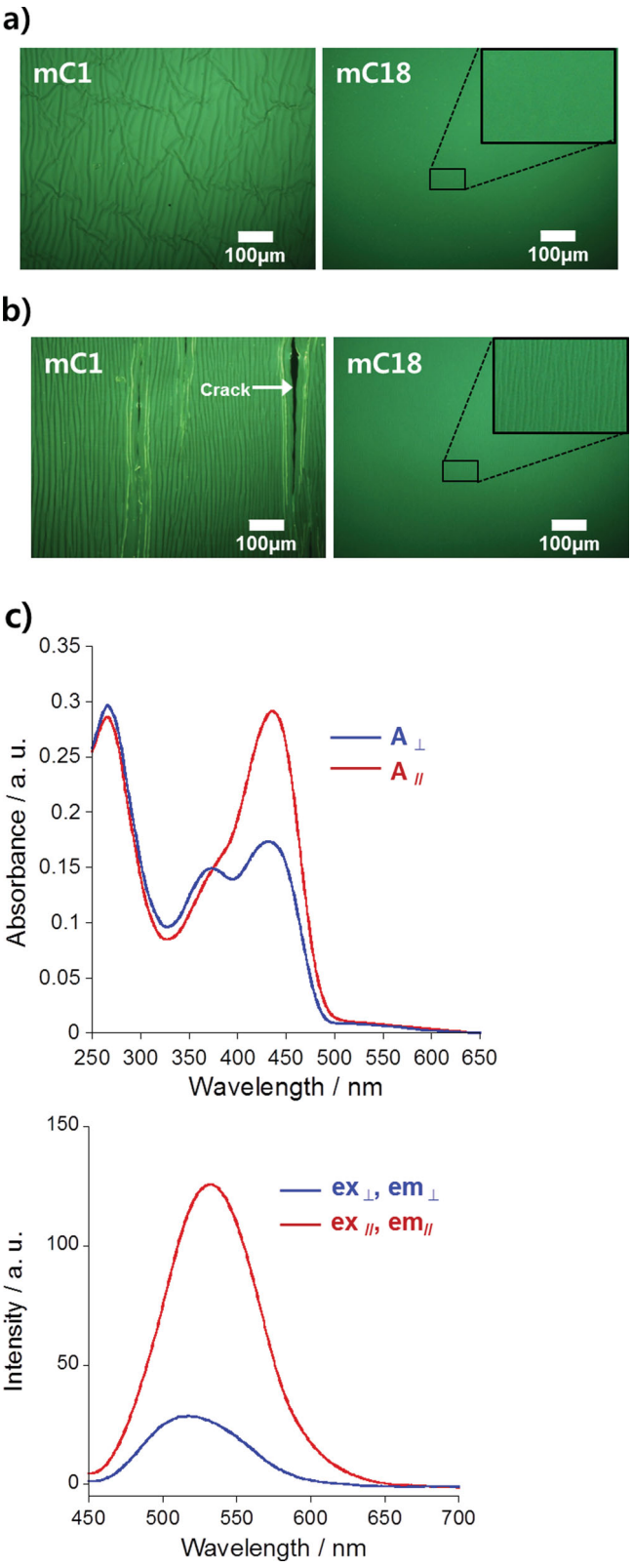

Figure 10. Fluorescent microscopy images of the mC1 and mC18 films spin-coated on PDMS substrates (film thickness ≈200 nm) : a) as-prepared, b) after stretching (strain 200%) and relaxing the films 50 times. c) Polarized UV-vis absorption and FL emission spectra (excited at 420 nm) of the elastomer-supported mC18 film when stretched at 200%.

3. Conclusion

This paper reported a strategic softening technology that makes a generally stiff and rigid π-conjugated polymer a very soft gum-like polymer in the bulk solid. The PDPA derivative with a highly twisted backbone and nonplanar geometry is an excellent candidate for developing a gum-like conjugated polymer. The alkyl side chain length and its substitution position are very important for introducing gum-like behavior and enhanced FL emission. The drawn free-standing film and stretched elastomer-supported film of the gum polymer exhibits large optical anisotropy in FL emission. In particular, the gum polymer film on the PDMS substrate accommodated very large strain without cracking or delamination. Highly branched alkyl chains and/or a much larger substitution number will be more effective in the development of softer PDPA derivatives with a higher emission efficiency. The branched alkyl groups might wrap the rigid backbones more effectively and reduce the elastic modulus of the polymer to completely isolate the polymer chains, even in the bulk solid, and fully relax the intramolecular stack structure. Further molecular designs for softening the PDPA-based π-conjugated polymers to oils and making the oily polymers stretchable elastomers in a single bulk component via a chemical cross-linking reaction are currently in development.

4. Experimental Section

Materials: The PDPA derivatives of pC1, pC18, and mC1 were synthesized using the methodology reported elsewhere.[20] A monomer of mC18 was prepared using the same technique, using 1,3-dibromobenzene and chlorodimethyl(octadecyl)silane as the starting materials. Yield 62.6%, purity >99% (^{1}H NMR), clear liquid. ^{1}H NMR (400 MHz, $CDCl_3$, δ): 7.2–7.8 (m, 9H, Ar H), 0.75–1.25 (t, 37H, octadecyl), 0.23 (s, 6H, dimethyl) ppm. Polymerization of mC18 was carried out using the methodology reported elsewhere[20] to provide an orange gum polymer with a yield of 70%. All polymers were purified several times by Soxhlet extraction with methanol and acetone in sequence. All reagents and solvents were purchased from Sigma-Aldrich.

Measurements: The weight-average molecular weight (M_w) and number-average molecular weight (M_n) of the PDPA derivatives were evaluated by gel permeation chromatography (GPC, Shimadzu A10 instruments, Polymer Laboratories, PLgel Mixed-B (300 mm in length) as the column, and HPLC-grade tetrahydrofuran as the eluent at 40 °C), based on a calibration with polystyrene standards. UV absorption spectroscopy was performed on a JASCO V-650 spectrophotometer, and the photoluminescence spectra were recorded on a JASCO FP-6500 spectrofluorometer at an excitation wavelength of 420 nm and a scanning rate of 100 nm/min at room temperature (excitation light source: xenon lamp; excitation light power: 1.73 μW cm^{-2}). Polarized UV-vis absorption and photoluminescence spectroscopy were performed using the same spectrometers with the corresponding JASCO polarizer/analyzer units, respectively. The fluorescence pictures and videos of the PDPA derivatives were taken with a digital camera (Canon PowerShot A2000 IS) at an excitation wavelength of >365 nm. The time-resolved emission spectra were measured on a streak camera using a femtosecond laser pulse from an optical parametric amplifier (Hamamatsu Photonics C4780). The width of the laser pulse was approximately 3 nm and the repetition rate was 5 ns. These measurements were carried out at room temperature in air. XRD (PANalytical X`Pert PRO-MPD) was performed at room temperature at the Korea Basic Science Institute (Daegu). The samples were mounted directly into the diffractometer. The experiment was carried out using Cu K α (1.54 Å) radiation operating at 40 kV and 25 mA. Differential scanning calorimetry (DSC, TA Instruments Q2000) was performed under pure nitrogen gas at heating and cooling rates of 10 °C min^{-1}. Dynamic thermo-mechanical analysis (DTMA, TA Instruments TMA Q400EM) was performed in tension mode using an oscillating force ramp. All samples were prepared by the solvent casting on the Teflon plate, the sample size was 26 mm (L) × 35 mm (T) × 4.7 mm (W). The initiated force was 0.05N at a frequency of 1 Hz (heating rate: 10 °C min^{-1}, under nitrogen gas). The rheological behavior was measured by AR2000-ex (TA instruments, stress-controlled rheometer) with a 40 mm cone-and-plate. The frequency sweep tests were conducted at room-temperature (25 °C). The concentration of the samples in a 1,2-dichlorobenzene solution was 5×10^{-2} mol L^{-1} in repeat unit. The photoluminescence quantum yields of the PDPA derivatives in a toluene solution were determined relative to a quinine sulfate solution in a 1 N H_2SO_4 at room-temperature, assuming a quantum yield of 0.546 when excited at 365 nm. The solid state quantum yields were obtained relative to 9,10-diphenylanthracence in poly(methyl methacrylate) (PMMA) matrix (Φ_{re} = 0.83, 10^{-3} M).

Supporting Information

Supporting Information is available from the Wiley Online Library or from the author.

Acknowledgements

This work was supported by the Basic Science Research Program through the National Research Foundation of Korea (NRF) grants funded by the Korea government (MEST) (2011–0016681, 2008–0062617). This study was also supported by the Research Fund of the National Forensic Service of Korea. This research was supported by a grant from the R&D Program (nanotechnology convergence project for commercialization and platform, Grant No.10036099) funded by the Ministry of Knowledge Economy (MKE), Republic of Korea. Also, the authors are deeply thankful to all interested persons of MKE and KEIT (Korea Evaluation Institute of Industrial Technology).

Received: August 12, 2013
Revised: September 3, 2013
Published online: October 14, 2013

[1] a) M. Armand, F. Endres, D. R. MacFarlane, H. Ohno, B. Scrosati, *Nat. Mater.* **2009**, *8*, 621; b) A. W. Perriman, A. P. S. Brogan, H. Colfen, N. Tsoureas, G. R. Owen, S. Mann, *Nat. Chem.* **2010**, *2*, 622; c) Y. Bai, Y. Cao, J. Zhang, M. Wang, R. Li, P. Wang, S. M. Zakeeruddin, M. Gratzel, *Nat. mater.* **2008**, *7*, 626; d) H. -J. Koo, J.-H. So, M. D. Dickey, O. D. Velev, *Adv. Mater.* **2011**, *23*, 3559; e) T. Torimoto, T. Tsuda, K. Okazaki, S. Kuwabata, *Adv. Mater.* **2010**, *22*, 1196; f) V. K. Thorsmolle, D. Topgaard, J. C. Brauer, S. M. Zakeeruddin, B. Lindman, M. Gratzel, J.-E. Moser, *Adv. Mater.* **2012**, *24*, 781; g) S. C. Warren, M. J. Banholzer, L. S. Slaughter, E. P. Giannelis, F. J. DiSalvo, U. B. Wiesner, *J. Am. Chem. Soc.* **2006**, *128*, 12074; h) E. M. Maya, J. S. Shirk, A. W. Snow, G. L. Roberts, *Chem. Commun.* **2001**, 615; i) S. Maruyama, K. Sato, H. Iwahashi, *Chem. Lett.* **2010**, *39*, 714; j) A. Nowak-Krol, D. Gryko, D. T. Gryko, *Chem. Asian J.* **2010**, *5*, 904; k) T. Michinobu, T. Nakanishi, J. P. Hill, M. Funahashi, K. Ariga, *J. Am. Chem. Soc.* **2006**, *128*, 10384; l) S. Hirata, K. Kubota, H. H. Jung, O. Hirata, K. Goushi, M. Yahiro, C. Adachi, *Adv. Mater.* **2011**, *23*, 889.

[2] a) S. S. Babu, J. Aimi, H. Ozawa, N. Shirahata, A. Saeki, S. Seki, A. Ajayaghosh, H. Mohwald, T. Nakanishi, *Angew. Chem. Int. Ed.* **2012**, *51*, 3391; b) S. S. Babu, M. J. Hollamby, J. Aimi, H. Ozawa,

A. Saeki, S. Seki, K. Kobayashi, K. Hagiwara, M. Yoshizawa, H. Mohwald, T. Nakanishi, *Nat. Commun.* **2013**, *4*, 1969.

[3] a) J. L. Bredas, R. R. Chance, *Conjugated polymeric Materials: Opportunites in Electronics, Optolelectronics, and Molecular Electronics*, Kluwer Academic, Dordrecht, Netherlands **1990**, pp. 1–10; b) J. A. Osaheni, S. A. Jenekhe, *Chem. Mater.* **1992**, *4*, 1282; c) J. Cornil, D. A. dos Santos, X. Crispin, R. Silbey, J. L. Bredas, *J. Am. Chem. Soc.* **1998**, *120*, 1289; d) A. Kraft, A. C. Grimsdale, A. B. Holmes, *Angew. Chem. Int. Ed.* **1998**, *37*, 403; e) U. H. F. Bunz, *Chem. Rev.* **2000**, *100*, 1605; f) M. S. Taylor, T. M. Swager, *Angew. Chem. Int. Ed.* **2007**, *46*, 8480; g) C. R. Grenier, W. Pisula, T. J. Joncheray, K. Muller, J. R. Reynolds, *Angew. Chem. Int. Ed.* **2007**, *46*, 714; h) U. H. F. Bunz, *Macromol, Rapid Commun.* **2009**, *30*, 772.

[4] a) J. J. M. Halls, C. A. Walsh, N. C. Greenham, E. A. Marseglia, R. H. Friend, S. C. Moratti, A. B. Holmes, *Nature* **1995**, *376*, 498; b) G. Li, V. Shrotriva, J. Huang, Y. Yao, T. Moriarty, K. Emery, Y. Yang, *Nat. Mater.* **2005**, *4*, 864; c) Y. Kim, S. Cook, S. M. Tuladhar, S. A. Choulis, J. Nelson, J. R. Durrant, D. D. C. Bradley, M. Giles, I. McCulloch, C. S. Ha, M. Ree, *Nat. Mater.* **2006**, *5*, 197; d) S. Gunes, H. Beugebauer, N. S. Sariciftci, *Chem. Rev.* **2007**, *107*, 1324; e) B. C. Thomson, J. M. J. Frechet, *Angew . Che m. Int. Ed.* **2008**, *47*, 58; f) B. S. Ong, Y. Wu, P. Liu, S. Gardner, *J. Am. Chem. Soc.* **2004**, *126*, 3378; g) L. L. Chua, J. Zaumseil, J.-F. Chang, E. C. W. Ou, P. K. H. Ho, H. Sirringhaus, R. H. Friend, *Nature* **2005**, *434*, 194; h) M. Heeney, C. Bailey, K. Genevicius, M. Shlunov, D. Sparrowe, S. Tierney, I. McCulloch, *J. Am. Chem. Soc.* **2005**, *127*, 1078; i) Y. D. Park, D. H. Kim, J. A. Lim, J. H. Cho, Y. Jang, W. H. Lee, J. H. Park, K. Cho, *J. Phys. Chem. C* **2008**, *112*, 1705.

[5] a) I. F. Perepichka, D. F. Perepichka, H. Meng, F. Wudl, *Adv. Mater.* **2005**, *17*, 2281; b) S. R. Amrutha, M. J. Jayakannan, *J. Phys. Chem. B* **2006**, *110*, 4083; c) L. Sun, P. Wang, H. Jin, X. Fan, Z. Shen, X. Xhen, G.-F. Zhou, *J. Polym. Sci. A: Polym. Chem.* **2008**, *46*, 7173; d) S. R. Amrutha, M. Jayakannan, *J. Phys. Chem. B* **2008**, *112*, 1119; e) T. Sato, D. -L. Jiang, T. Aida, *J. Am. Chem. Soc.* **1999**, *121*, 10658; f) B. C. Englert, M. D. Smith, K. I. Hardcastle, U. H. F. Bunz, *Macromolecules* **2004**, *37*, 8212; g) Y. K. Kwon, H. S. Kim, H. J. Kim, J. H. Oh, H. S. Park, Y. S. Ko, K. B. Kim, M. S. Kim, *Macromolecules* **2009**, *42*, 887.

[6] a) I. Nurulla, T. Morikita, H. Fukumoto, T. Yamamoto, *Macromol. Chem. Phys.* **2001**, *202*, 2335; b) M. Moroni, J. Le Moigne, *Macromolecules* **1994**, *27*, 562; c) F. C. Krebs, M. Jorgensen, *Macromolecules* **2003**, *36*, 4374; d) M. Knaapila, R. Stepanyan, B. P. Lyons, M. Torkkeli, A. P. Monkman, *Adv. Funct. Mater.* **2006**, *16*, 599; e) W.-P. Hsu, K. Levon, K.-S. Ho, A. S. Myerson, T. K. Kwei, *Macromolecules* **1993**, *26*, 1318; f) M. D. Curtis, J. I. Nanos, H. Moon, W. S. Jahng, *J. Am. Chem. Soc.* **2007**, *129*, 15072; g) S. H. Chen, A. C. Su, C. H. Su, *Macromolecules* **2005**, *38*, 379.

[7] a) D.-H. Kim, J.-H. Ahn, W. M. Choi, H.-S. Kim, T.-H. Kim, J. Song, Y. Y. Huang, Z. Liu, C. Lu, J. A. Rogers, *Science* **2008**, *320*, 507; b) T. Sekitani, Y. Noguchi, K. Hata, T. Fukushima, T. Aida, T. Someya, *Science* **2008**, *321*, 1468; c) J. A. Rogers, T. Someya, Y. Huang, *Science* **2010**, *327*, 1603; d) T. S. Hansen, O. Hassager, N. B. Larsen, *Adv. Funct. Mater.* **2007**, *17*, 3069; e) F. Carpi, G. Gallone, F. Galantini, D. D. Rossi, *Adv. Funct. Mater.* **2008**, *18*, 235; f) A. J. Granero, P. Wagner, K. Wagner, J. M. Razal, G. G. Wallace, M. Panhuis, *Adv. Funct. Mater.* **2011**, *21*, 955.

[8] a) S. V. Frolov, A. Fujii, D. Chinn, M. Hirohata, R. Hidayat, M. Teraguchi, T. Masuda, *Adv. Mater.* **1998**, *10*, 869; b) R. Hidayat, S. Tatsuhara, D. W. Kim, M. Ozaki, K. Yoshino, M. Teraguchi, T. Masuda, *Phys. Rev. B* **2000**, *61*, 10167; c) H. Ghosh, A. Shukla, S. Mazumdar, *Phys. Rew. B* **2000**, 62, 12763; d) A. Shukla, H. Ghosh, S. Mazumdar, *Synth. Met.* **2001**, *116*, 87; e) R. Hidayat, A. Fujii, M. Ozaki, M. Teraguchi, T. Masuda, K. Yoshino, *Synth. Met.* **2001**, *119*, 597; f) A. Fujii, R. Hidayat, T. Sonoda, T. Fujisawa, M. Ozaki, Z. V. Vardeny, M. Teraguchi, T. Masuda, K. Yoshino, *Synth. Met.* **2001**, *116*, 95; g) A. Shukla, *Chem. Phys.* **2004**, *300*, 177.

[9] a) J. W. Y. Lam, B. Z. Tang, *Acc. Chem. Res.* **2005**, *38*, 745; b) J. W. Y. Lam, Y. Dong, C. C. W. Law, Y. Dong, K. K. L. Cheuk, L. M. Lai, Z. Li, J. Sun, H. Chen, Q. Zheng, H. S. Kwok, M. Wang, X. Feng, J. Shen, B. Z. Tang, *Macromolecules* **2005**, *38*, 3290.

[10] a) G. Kwak, M. Minaguchi, T. Sakaguchi, T. Masuda, M. Fujiki, *Chem. Mater.* **2007**, *19*, 3654; b) G. Kwak, M. Minaguchi, T. Sakaguchi, T. Masuda, M. Fujiki, *Macromolecules* **2008**, *41*, 2743; c) G. Kwak, W.-E. Lee, H. Jeong, T. Sakaguchi, M. Fujiki, *Macromolecules* **2009**, *42*, 20.

[11] a) W.-E. Lee, J.-W. Kim, C.-J. Oh, T. Sakaguchi, M. Fujiki, G. Kwak, *Angew. Chem. Int. Ed.* **2010**, *49*, 1406; b) W.-E. Lee, C.-J. Oh, G.-T. Park, J.-W. Kim, H.-J. Choi, T. Sakaguchi, M. Fujiki, A. Nakao, K. Shinohara, G. Kwak, *Chem. Commun.* **2010**, *46*, 6491; c) W.-E. Lee, C.-L. Lee, T. Sakaguchi, M. Fujiki, G. Kwak, *Macromolecules* **2011**, *44*, 432; d) W.-E. Lee, Y.-J. Jin, L.-S. Park, G. Kwak, *Adv. Mater.* **2012**, *24*, 5604.

[12] a) S. I. Kolesnikov, Z. I. Syunyaev, *Zhur. Prikl. Khim.* **1985**, *58*, 2267; b) P. Barbillon, L. Schuffenecker, J. Dellacherie, D. Balesdent, M. Dirande, *J. Chim. Phys. Phys.-Chim. Biol.* **1991**, *88*, 91.

[13] a) K.-Q. Zhao, C. Chen, H. Monobe, P. Hu, B.-Q. Wang, Y. Shimizu, *Chem. Commun.* **2011**, *47*, 6290; b) T. Cardinaels, K. Lava, K. Goossens, S. V. Eliseeva, K. Binnemans, *Langmuir* **2011**, *27*, 2036.

[14] L. J. Fetters, D. J. Lohse, D. Richter, T. A. Witten, A. Zirkel, *Macromolecules* **1994**, *27*, 4639.

[15] L. G. Toy, K. Nagai, B. D. Freeman, I. Pinnau, Z. He, T. Masuda, M. Teraguchi, Y. P. Yampolskii, *Macromolecules* **2000**, *33*, 2516.

[16] a) R. I. Wolkowicz, W. C. Forsman, *Macromolecules* **1971**, *4*, 184; b) J. Klein, *Macromolecules* **1978**, *11*, 852; c) M. Rubinstein, A. N. Semenov, *Macromolecules* **2001**, *34*, 1058.

[17] a) M. Grell, D. D. C. Bradley, *Adv. Mater.* **1999**, *11*, 895; b) M. Grell, W. Knoll, D. Lupo, A. Meisel, T. Miteva, D. Neher, H.-G. Nothofer, U. Scherf, A. Yasuda, *Adv. Mater.* **1999**, *11*, 671; c) M. Aldred, A. E. A. Contoret, S. Farrar, S. M. Kelly, D. Mathieson, M. O'Neill, W. C. Tsoi, P. Vlachos, *Adv. Mater.* **2005**, *17*, 1368; d) M. O'Neill, S. M. Kelly, *Adv. Mater.* **2003**, *14*, 1135; e) H. Hayasaka, K. Tamura, K. Akagi, *Trans. Mater. Res. Soc. Jpn.* **2007**, *32*, 395; f) A. Ohira, T. M. Swager, *Macromolecules* **2007**, *40*, 19; g) W. Molenkamp, M. Watanabe, H. Miyata, S. H. Tolbert, *J. Am. Chem. Soc.* **2004**, *126*, 4476.

[18] a) D. J. Lipomi, B. C.-K. Tee, M. Vosgueritchian, Z. Bao, *Adv. Mater.* **2011**, *23*, 1771; b) Z. Yu, X. Niu, Z. Liu, Q. Pei, *Adv. Mater.* **2011**, *23*, 3989; c) T. Sekitani, T. Someya, *Adv. Mater.* **2010**, *22*, 2228; d) S. C. B. Mannsfeld, B. C.-K. Tee, R. M. Stoltenberg, C. V. H.-H. Chen, S. Barman, B. V. O. Muir, A. N. Sokolov, C. Reese, Z. Bao, *Nat. Mater.* **2010**, *9*, 859; e) T. Sekitani, H. Nakajima, H. Maeda, T. Fukushima, T. Aida, K. Hata, T. Someya, *Nat. Mater.* **2009**, *8*, 494.

[19] a) N. Bowden, S. Brittain, A. G. Evans, J. W. Hutchinson, G. M. Whitesides, *Nature* **1998**, *393*, 146; b) C. Yu, C. Masarapu, J. Rong, B. Wei, H. Jiang, *Adv. Mater.* **2009**, *21*, 4793; c) D. Tahk, H. H. Lee, D.-Y. Khang, *Macromolecules* **2009**, *42*, 7079; d) H. Jiang, D.-Y. Khang, Z. Song, Y. Sun, Y. Huang, J. A. Rogers, *Proc. Natl. Acad. Sci. U. S. A.* **2007**, *104*, 15607; e) D.-Y. Khang, H. Jiang, Y. Huang, J. A. Rogers, *Science* **2006**, *311*, 208.

[20] a) K. Tsuchihara, T. Masuda, T. Higashimura, *J. Am. Chem. Soc.* **1991**, *113*, 8548; b) T. Sakaguchi, K. Yumoto, M. Shiotsuki, F. Sanda, M. Yochikawa, T. Masuda, *Macromolecules* **2005**, *38*, 2704.